

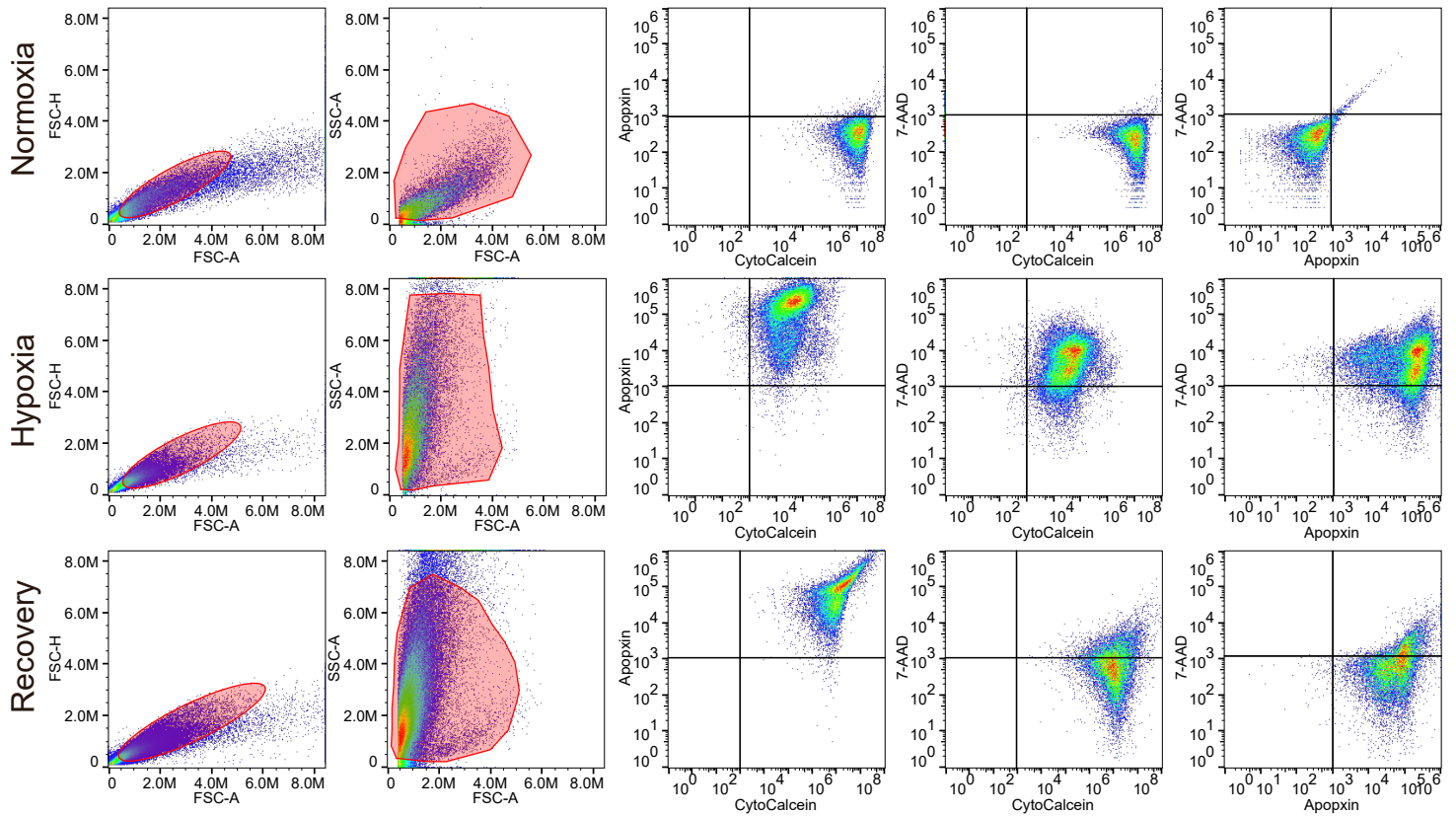
Supplemental Information

Improved post-stroke spontaneous recovery

by astrocytic extracellular vesicles

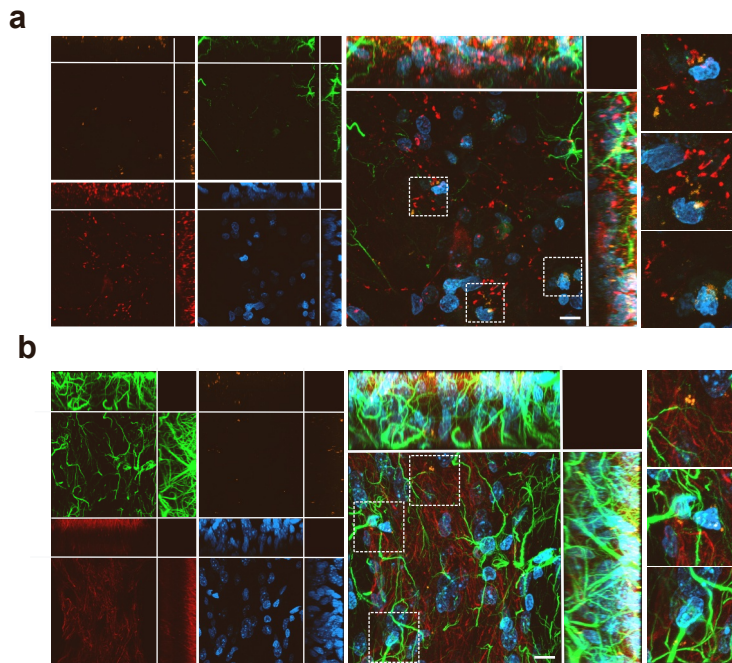
Yessica Heras-Romero, Axayacatl Morales-Guadarrama, Ricardo Santana-Martínez, Isaac Ponce, Ruth Rincón-Heredia, Augusto César Poot-Hernández, Araceli Martínez-Moreno, Esteban Urrieta, Berenice N. Bernal-Vicente, Aura N. Campero-Romero, Perla Moreno-Castilla, Nigel H. Greig, Martha L. Escobar, Luis Concha, and Luis B. Tovar-y-Romo

Supplementary Figure 1



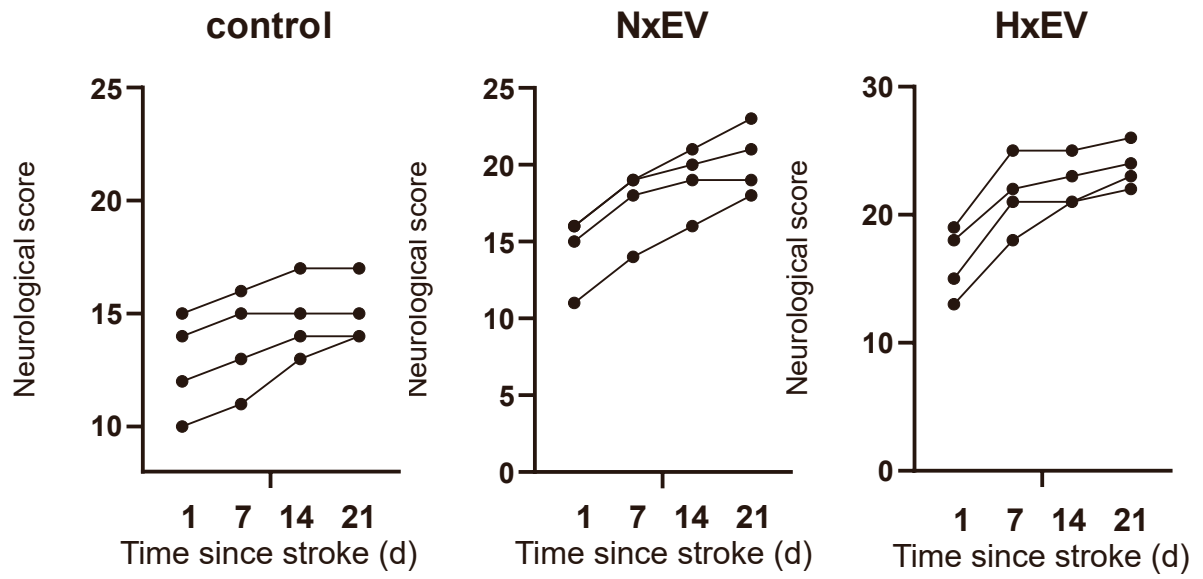
Supplementary Figure 1. Representative scattergrams showing flow cytometry for cell viability after hypoxia. Gating for singlets (FSC-A/FSC-H) and granularity (FSC-A/SSC-A) are shown on the left. Analysis of CytoCalcein, Apoptin, and 7-AAD markers in astrocytes cultured under normoxia, hypoxia (6 h), and recovery (6 h hypoxia followed by 42 h normoxia) conditions are shown on the right. The dot plots of Apoptin vs. CytoCalcein, 7-AAD vs. CytoCalcein, and 7-AAD vs. Apoptin show resolution of live, injured, and dead cell populations.

Supplementary Figure 2



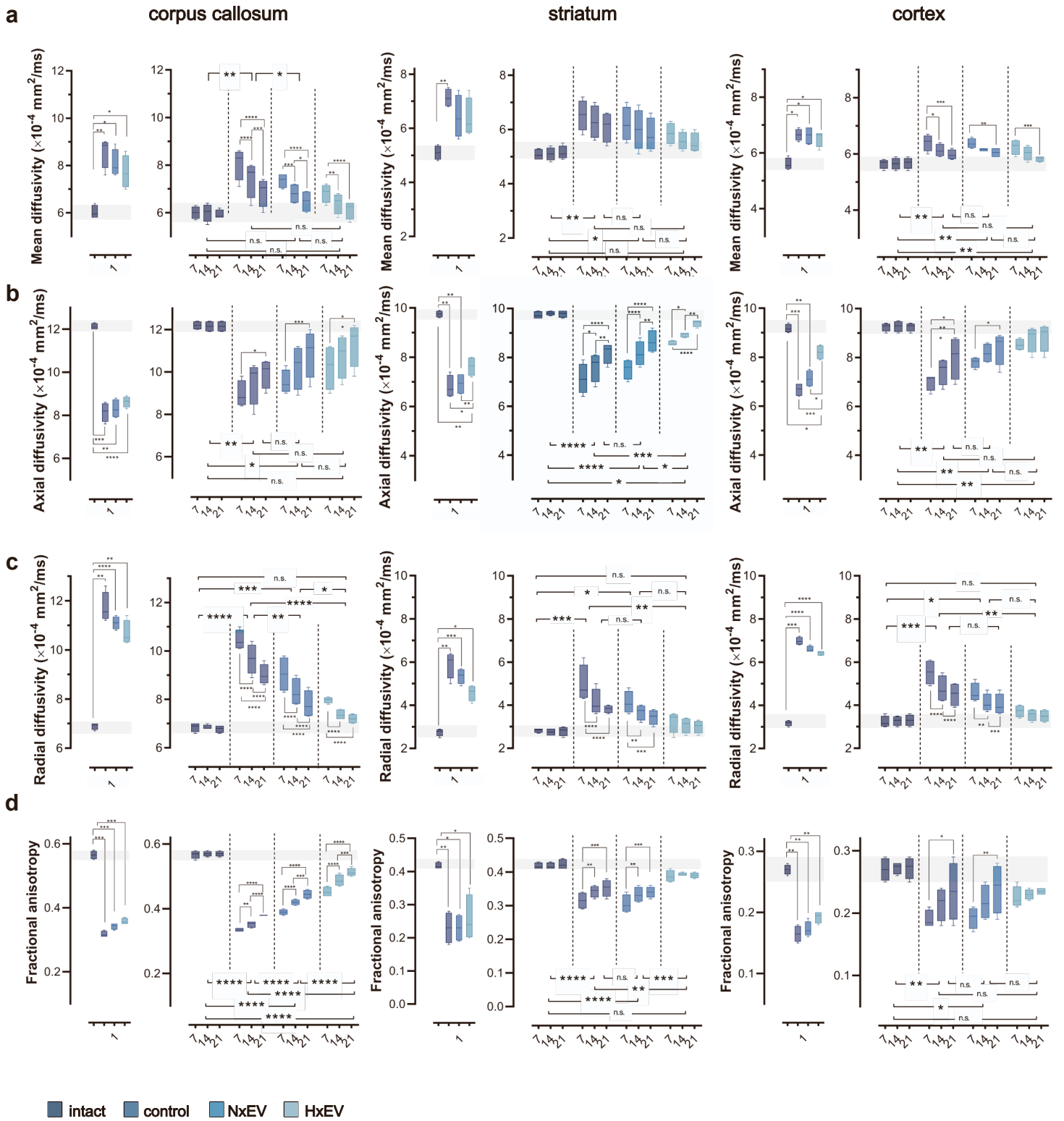
Supplementary figure 2 Distribution of EVs stained with PKH26 (orange) at 24 h after i.c.v. injection in the brain of stroke-challenged rats in the striatum **(a)** and motor cortex **(b)**. EVs internalize in neurons (MAP2; red) and astrocytes (GFAP; green) and preferentially localized to perinuclear (DAPI; blue) regions. Dotted squares demark regions where EVs localize. Images are maximum projections of a Z-stack of 20 optical slices showing the orthogonal planes, and nuclei are stained with DAPI (blue), scale bar equals 10 μm.

Supplementary Figure 3



Supplementary figure 3. Spontaneous recovery trends of individual animals in each group, assessed at 1, 7, 14, and 21 days post-stroke.

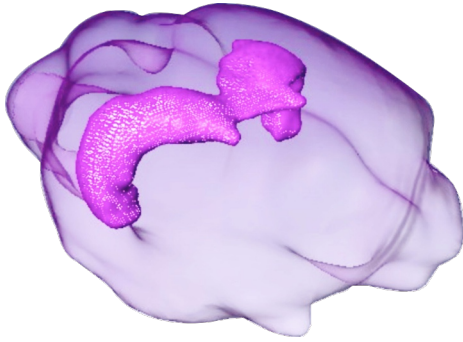
Supplementary Figure 4



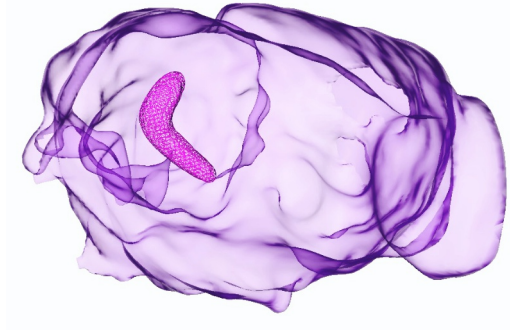
Supplementary figure 4. Evolution of DTI parameters in the contra-lesional hemisphere. **(a)** mean diffusivity, **(b)** axial diffusivity, **(c)** radial diffusivity, and **(d)** fractional anisotropy were determined from diffusion tensor imaging (DTI) of the contralateral corpus callosum (left column), striatum (middle column), and motor cortex (right column) at 1, 7, 14 and 21 days post-stroke. Boxplots on day 1 show the alterations caused by the stroke in all four DTI parameters; no statistical differences exist between stroke-challenged animals treated with vehicle (control) and those that received EVs 30 min after the initiation of reperfusion. Boxplots show the min and max values within each group, the dispersion span from Q1 to Q3, and the mean, n=4. The shaded horizontal bar in each plot marks the span of ± 1 S.D. of the intact group baseline values. Statistical differences of the recovery trend are indicated among groups with repeated measures two-way ANOVA followed by Tukey's post hoc, and changes over time within each group are also indicated with two-way ANOVA followed by Tukey's post hoc. * $p < 0.05$, ** $p < 0.01$, *** $p < 0.001$ and **** $p < 0.0001$.

Supplementary Figure 5

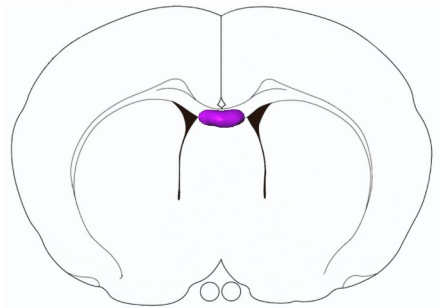
a



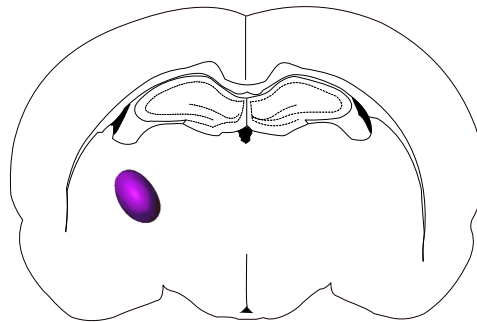
b



c

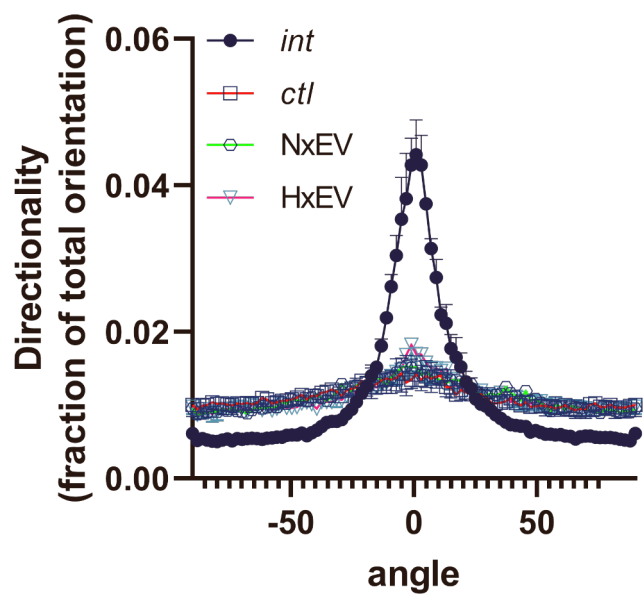


d



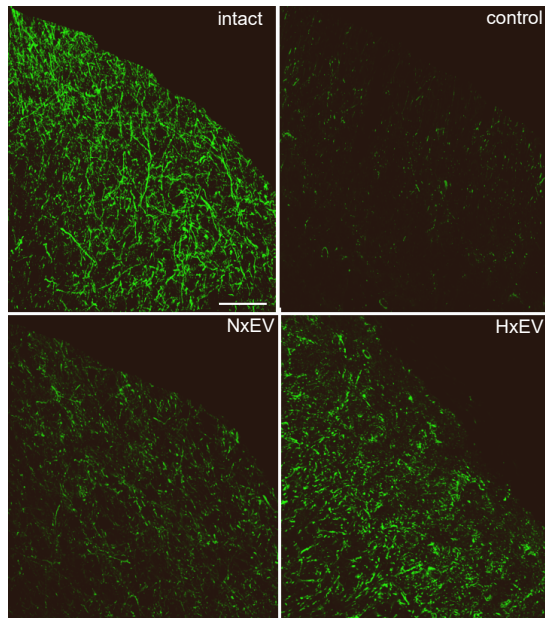
Supplementary figure 5. Diffusion tensor imaging-based tissue segmentation rendering of the corpus callosum **(a)** and the corticostriatal tract **(b)** of the rat brain. Regions of interest where seeds used to initiate tractography were placed in the corpus callosum (AP 0.2 from Bregma) **(c)** and corticostriatal (AP -2.8 from Bregma) **(d)** tracts.

Supplementary Figure 6



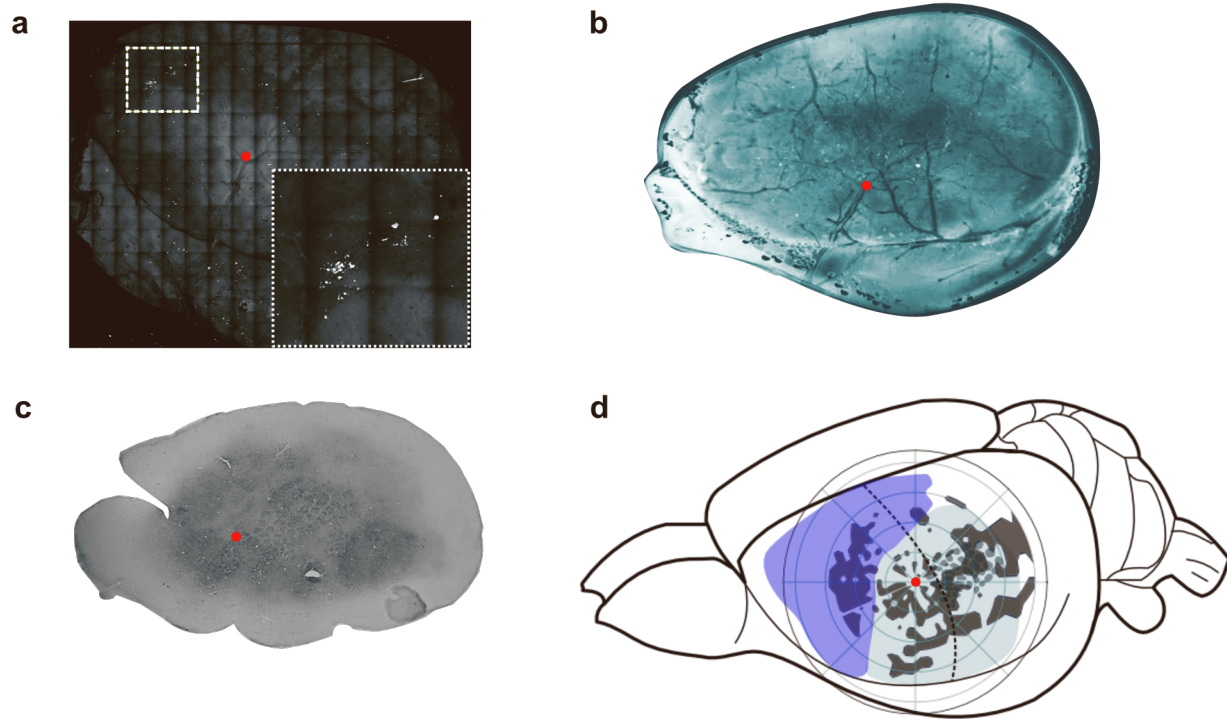
Supplementary figure 6. Analysis of the directionality of MAP-2 immunolabeled fibers in the striatum 21 days after stroke. The EV-induced increases in fiber staining did not restore the directionality of the fibers after stroke.

Supplementary Figure 7



Supplementary figure 7. Representative confocal micrographs of cortical labeling in animals injected in the dorsal striatum with the cholera toxin subunit B, which is retrogradely transported through the axonal system. Injections were made on day 14 after stroke and followed the fluorescent label's localization in the innervated cortical regions at day 21 post-stroke. Scale bar equals 50 μm .

Supplementary Figure 8



Supplementary figure 8. Mapping of the cortical axonal projections from the dorsal striatum was made by superposing the panoramic two-photon image (**a**) where the vasculature can be clearly appreciated, with the ink-stained flattened cortex showing the superficial cortical vasculature (**b**) and the cytochrome c oxidase staining of the barrel cortex (**c**). The red dot indicates the exact anatomical localization at the first branch split of the M4 segment in the MCA's superior trunk and its relative position to the barrel cortex. This anatomical location was designated as the origin (0,0 coordinate) for polar plots (**d**).

Supplementary video 1. Extracellular vesicles in the contralateral striatum 24 h after i.c.v. injection. The animation shows a confocal reconstruction of maximum projections of a Z-stack of 20 optical slices in a striatal tissue section from a rat injected i.c.v. with EVs stained with PKH26 (orange). Neurons are identified by MAP2 staining in red, and astrocytes are labeled with GFAP in green. Cell nuclei are stained with DAPI in blue. Blue circles indicate the presence of external EVs near the nuclei of neurons and astrocytes.

Supplementary video 2. Sensory test: stimulation of vibrissae 14 days after stroke. Two rats administered with vehicle (control) or HxEV are stimulated by a gentle stroke of the vibrissae 14 days after MCAO. The rat on the right that received HxEV is more responsive to the stimulation than the control one.

Supplementary video 3. Infarct volume and tractography 21 days after stroke. A representative MRI reconstruction of the infarct lesion for each experimental condition is presented 21 days after stroke. The animals treated with NxEV or HxEV exhibit a decreased lesion volume. Representative tractographies generated from DTI imaging for each experimental condition show an enhanced axonal recovery in animals that received HxEV and NxEV compared with the control animal injected with vehicle only.